A R C H I V E S O F M E T A L L U R G Y A N D M A T E R I A L S
Volume 56 2011 Issue 4
DOI: 10.2478/v10172-011-0125-6

J. DZIK*, H. BERNARD*, K. OSIŃSKA*, A. LISIŃSKA-CZEKAJ*, D. CZEKAJ*

SYNTHESIS, STRUCTURE AND DIELECTRIC PROPERTIES OF $Bi_{1-x}Nd_xFeO_3$

SYNTEZA, STRUKTURA I WŁAŚCIWOŚCI DIELEKTRYCZNE $Bi_{1-x}Nd_xFeO_3$

In the present study $Bi_{1-x}Nd_xFeO_3$ (x=0.1-0.4) ceramic powders were synthesized by the conventional mixed oxide method. Stoichiometric mixture of the powders was thermally analysed with Netzsch STA-409 system so parameters of the thermal treatment were determined. Morphology of the ceramic material was observed by scanning electron microscopy, whereas the crystalline structure was studied by X-ray diffraction method. It was found that chemical composition of the ceramic samples corresponds well to the initial stoichiometry of the ceramic powders. An increase in neodymium content caused a decrease in the average size of the ceramic grains. Crystalline structure of $Bi_{1-x}Nd_xFeO_3$ ceramics for $x \leqslant 0.2$ was decribed by rhombohedral symmetry whereas for $x \geqslant 0.3$ by orthorhombic symmetry. Dielectric properties were studied within a range of frequency ν=20Hz – 1MHz at room temperature by impedance spectroscopy. The Kramers-Kronig data validation test was employed in the present impedance data analysis. Impedance data were fitted to the corresponding equivalent circuit using the CNLS fitting method.

Keywords: BiFeO3, Nd3+ doping, ceramics, impedance, spectroscopy

W niniejszej pracy przedstawiono rezultaty badań poświęconych wytwarzaniu i charakterystyce właściwości ceramiki $Bi_{1-x}Nd_xFeO_3$(x=0.1-0.4). W oparciu o analizę termiczną (DTA) i termograwimetryczną (TG/DTG) dobrano warunki obróbki cieplnej stechiometrycznej mieszaniny tlenków wyjściowych (Bi_2O_3, Fe_2O_3 i Nd_2O_3). Morfologię przełamu wytworzonej ceramiki $Bi_{1-x}Nd_xFeO_3$ obserwowano przy użyciu skaningowego mikroskopu elektronowego (SEM). Obrazy SEM ceramiki $Bi_{1-x}Nd_xFeO_3$wykazały, że stężenie neodymu ma znaczący wpływ na rozrost ziarna. Wraz ze wzrostem zawartości neodymu, zmniejsza się wielkość ziarna. Analiza RTG otrzymanej ceramiki $Bi_{1-x}Nd_xFeO_3$ pozwoliła stwierdzić, że dla $x \leqslant 0{,}2$ układ przyjmuje strukturę romboedryczną, natomiast dla $x \geqslant 0{,}3$ strukturę wytworzonego materiału ceramicznego należy opisywać symetrią rombową.

Do badania zależności impedancji $|Z|$ i kąta przesunięcia fazowego φ w funkcji częstotliwości w zakresie od f= 10 Hz do f= 1 MHz zastosowano sterowany komputerowo miernik impedancji typu QuadTech-1920. Analizę danych eksperymentalnych przeprowadzono metodą CNLS. Dane eksperymentalne otrzymane w wyniku badania ceramiki poddano analizie zgodności danych z wykorzystaniem równań Kramersa-Kroninga.

1. Introduction

$BiFeO_3$ is an inorganic chemical compound with a perovskite-type structure. It is one of the most promising materials due to the multiferroic properties that it exhibits at room temperature. It is worth nothing a that the ability to exhibit the electric and magnetic polarization, creates a great application potential in the design of advance devices where we can utilize the ferroelectric and ferromagnetic properties in the same device [1,2].

$BiFeO_3$ is the most attractive single-phase multiferroic material because of its high phase transition temperatures – Curie temperature T=830°C and Neel temperature T=370°C [3,4]. $BiFeO_3$ is characterized with a weak magnetism at room temperature [5]. Inspite, bismuth ferrite has very a high ferroelectric-paraelectric transition temperature, bismuth ferrite possesses low dielectric constant (ε=92-100 kHz). Since electric and magnetic response is subjected to local structural distortion, ferroelectric and magnetoresistive behavior will almost certainly be interrelated through substituent elements. It seems to be promising to suppress the spatial non-uniformity of magnetic structure of bismuth ferrite by neodymium substitution for bismuth [6].

In an attempt to get improved properties, $BiFeO_3$ is subjected to doping with diamagnetic ions as well as rare-earth cations. By substituting rare-earth cations for

* UNIVERSITY OF SILESIA, DEPARTMENT OF MATERIALS SCIENCE, 41-200 SOSNOWIEC, 2 ŚNIEŻNA STR., POLAND

A-site Bi^{3+} ion in the nominal $BiFeO_3$ composition, one can effectively modulate the crystal structure parameters of $BiFeO_3$, destroy the space - modulated spin structure, and release the measurement of weak ferromagnetism [7]. Neodymium substitution for bismuth is promising to suppress the spatial non-uniformity of magnetic structure of $BiFeO_3$.

It is worth noting that the difficulties in synthesizing of pure phase $BiFeO_3$ are well known. Therefore, a goal of the present paper was to synthesize and fabricate $Bi_{1-x}Nd_xFeO_3$ (x=0.1, 0.2, 0.3 and 0.4) ceramics by solid state reaction as well as investigate crystalline structure, microstructure, chemical composition and dielectric properties of the Nd-modified bismuth ferrite by impedance spectroscopy.

2. Experimental

Ceramic samples of (1-x)$BiFeO_3$- x$NdFeO_3$(BNFO) solid solution for x=0.1, 0.2, 0.3 and 0.4 were synthesized by solid state reaction method, using Bi_2O_3 , Fe_2O_3, Nd_2O_3 oxides in appropriate proportions (mixed oxide method – MOM). The material was prepared according to equation (1):

$$(1-x)Bi_2O_3+xNd_2O_3 + Fe_2O_3 \rightarrow 2Bi_{1-x}Nd_xFeO_3 \quad (1)$$

The powders were first thoroughly mixed, pressed into pallets of d=10mm in diameter and h=2mm thick at p=300MPa and calcined at temperature T=750°C for t=10h. Next the material was milled in a wet medium and dried. The synthesized ceramic powder was then pressed and formed into pellets under pressure of p=600MPa. $Bi_{1-x}Nd_xFeO_3$ ceramics was sintered in air at temperature T=1000°C for t=24h.

Simultaneous thermal analysis, in which both thermal analysis (DTA) and mass change effects (TG and DTG) are measured concurrently on the same sample was used to investigate synthesis effects in the stoichiometric mixture of powders. The measurements were obtained with Netzsch STA409 thermal analyzer which is a combined DTA/TG/DTG system.

The morphology of BNFO ceramic samples was studied by scanning electron microscopy HITACHI S-4700. The structural analysis was performed by X-ray diffraction (XRD). The X-ray patterns were recorded in a 2Θ range from 10° to 110° with the X'Pert Pro diffractometer in the Θ-2Θ mode at room temperature using CoKα radiation, detector scan step $\Delta 2\Theta$=0.01° and a counting time t=7s. Analysis of the X-ray diffraction patterns of the ceramic powders was carried out using a computer program X'Pert HighScore Plus software (PANalytical B.V.). X'Pert HighScore Plus program has enabled us to perform a phase analysis, using the latest available ICSD database [8]. Microstructure and crystalline structure studies of BNFO ceramics were carried out at room temperature.

A QuadTech 1920 precision LCR meter was used to carry out the impedance measurements in a frequency range of ν=20Hz-1MHz. Experimental data of impedance spectroscopy were fitted to the corresponding equivalent circuit using the complex non - linear least squares method (CNLS)[9]. The validity of the fitting procedure was estimated according to the following methods: χ-squared and the weighted sum of squares, referred to as χ^2 and WSS [10].

3. Results and discussion

Powdered stoichiometric mixture of oxides forming $Bi_{1-x}Nd_xFeO_3$ solid solution was investigated by STA within the temperature range T=20-1000°C. Fig. 1 shows the traces of DTA, TG and DTG recorded at a heating rate of 10deg/min for $Bi_{0.7}Nd_{0.3}FeO_3$ ceramic powder. The monotonous process of the mass loss (TG curve) reaches a value of Δm=-2.1% at T=700°C. On the DTA curve an endothermic maxima (minima in the DTA curve) can be observed at T=356°C and T=633°C. As a as they correspond to the mass loss one can ascribe them to chemical reaction.

Fig. 2 shows scanning electron micrographs of BNFO sintered at T=1000°C for t=24h. In the figure one can see that neodymium concentration (x) has a significant influence on the grain growth. With an increase in the neodymium content (x) the grain size decreases.

The room temperature X-ray diffraction pattern of $Bi_{1-x}Nd_xFeO_3$ ceramic powder is shown in Fig.3. As a result of the structural analysis it was found that for $x \leqslant 0.2$ the experimental diffraction patterns corresponded to rhombohedral symmetry described with R3c (No.161) space group – typical for bismuth ferrite. For $x \geqslant 0.3$ it was found that the experimental diffraction patterns corresponded to orthorhombic structure described with Pnma (No. 62) space group that is typical for neodymium ferrite. Calculated unit cell parameters are shown in Table 1.

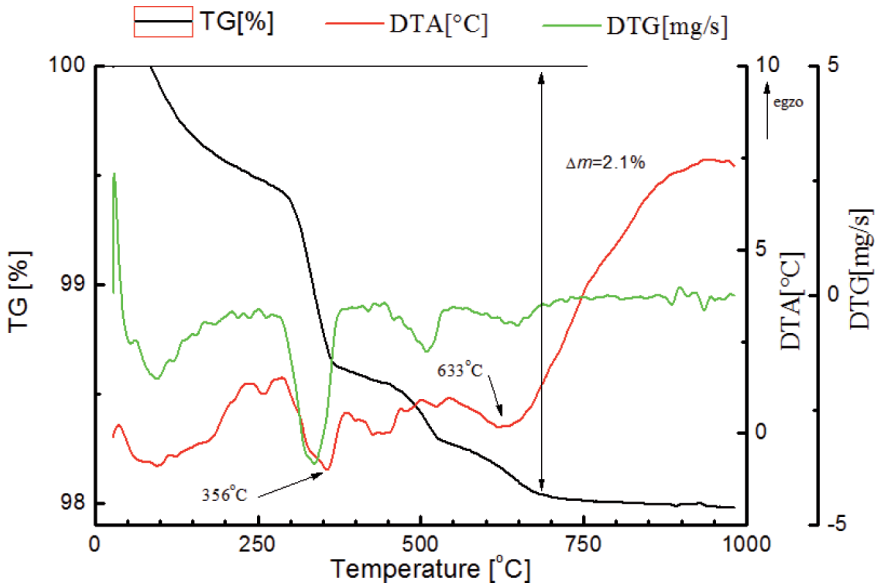

Fig. 1. DTA and TG curves for stoichiometric mixture of oxides used for fabrication of $Bi_{0.7}Nd_{0.3}FeO_3$ ceramics

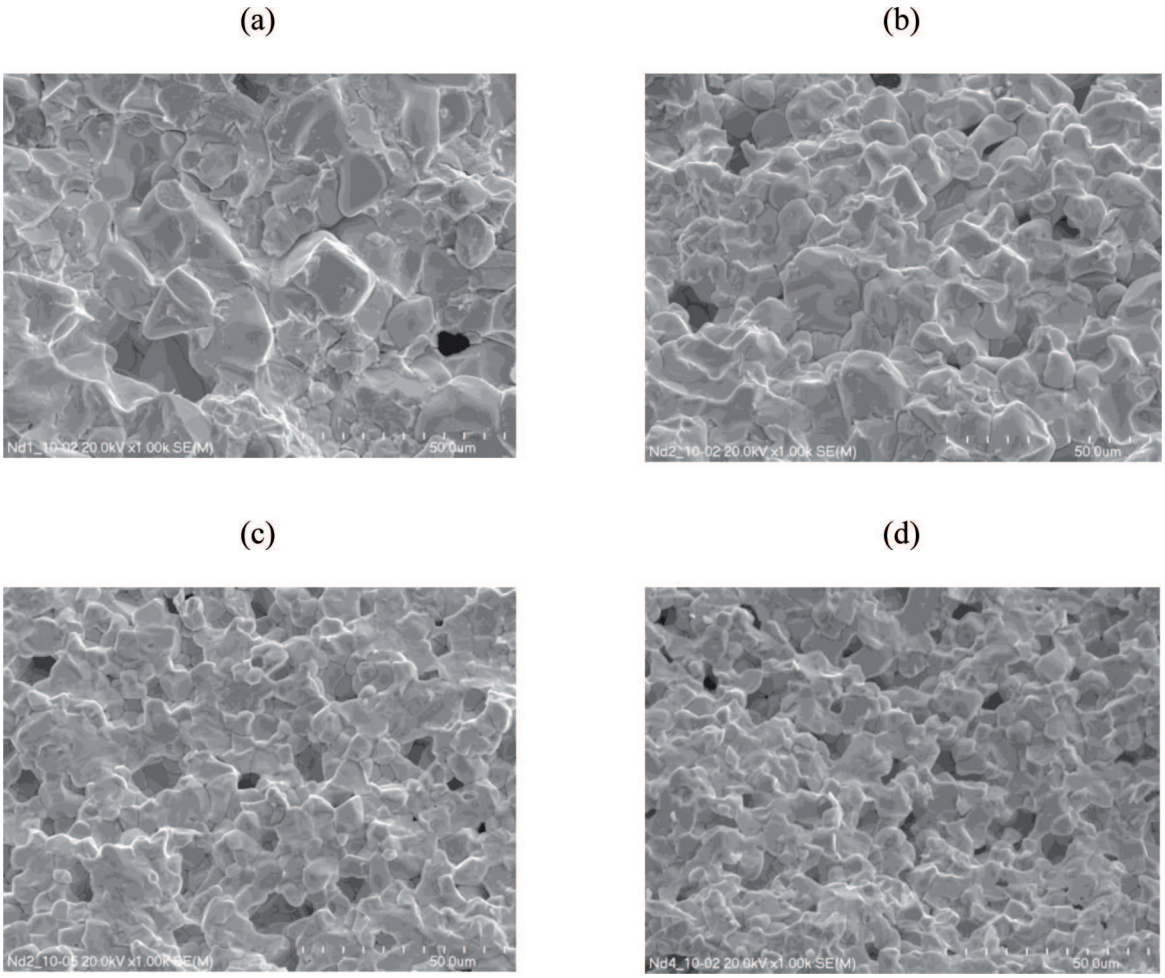

Fig. 2. SEM micrographs of $Bi_{1-x}Nd_xFeO_3$ sintered at T=1000^{0}C for t=24h, $Bi_{0.9}Nd_{0.1}FeO_3$ (a), $Bi_{0.8}Nd_{0.2}FeO_3$(b), $Bi_{0.7}Nd_{0.3}FeO_3$(c), $Bi_{0.6}Nd_{0.4}FeO_3$(d)

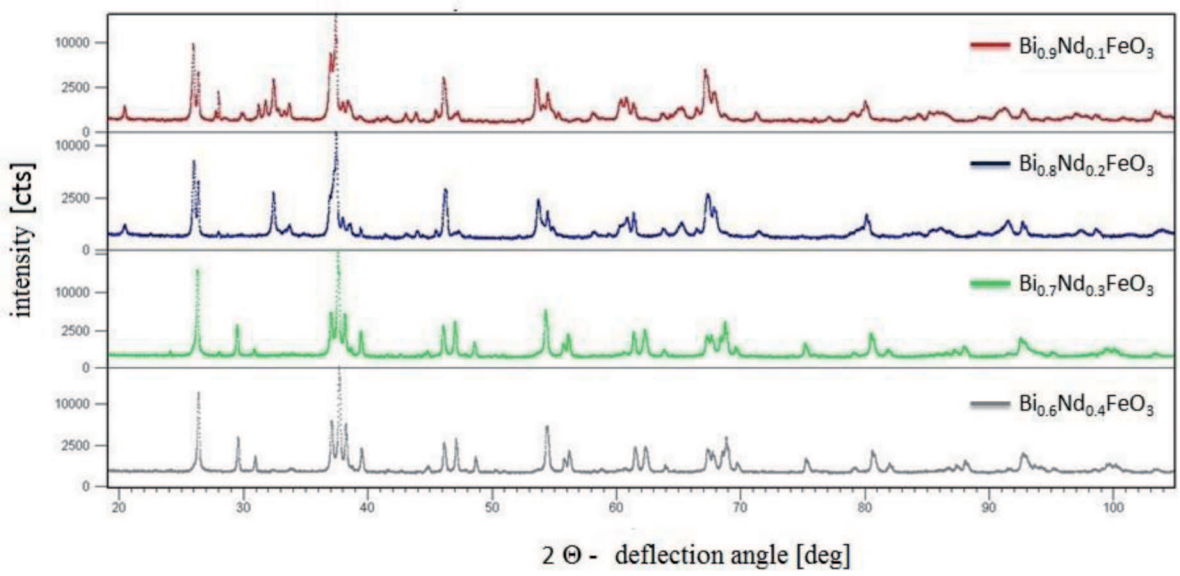

Fig. 3. Comparison of X-ray diffraction patterns for $Bi_{1-x}Nd_xFeO_3$ ceramics (Co-radiation)

TABLE 1

Cell parameters for $Bi_{1-x}Nd_xFeO_3$

Sample	a_0 [nm]	b_0 [nm]	c_0 [nm]	α [^{0}]	β [^{0}]	γ [^{0}]	$V\times10^6$ [pm^3]
$\mathbf{Bi_{0.9}Nd_{0.1}FeO_3}$	0.556	0.556	1.38	90	90	120	372.17
$\mathbf{Bi_{0.8}Nd_{0.2}FeO_3}$	0.556	0.556	1.383	90	90	120	371.35
$\mathbf{Bi_{0.7}Nd_{0.3}FeO_3}$	0.560	0.781	0.545	90	90	90	239.00
$\mathbf{Bi_{0.6}Nd_{0.4}FeO_3}$	0.561	0.780	0.544	90	90	90	238.75

Impedance spectroscopy is a powerful method of characterizing electrical properties of electroceramic materials [11,12]. The dielectric properties of BNFO were determined within a frequency range ν=20Hz-1MHz. It is commonly known [13,14] that the experimental data one can analyze in terms of four possible immitance functions, the impedance Z^*, the electric modulus M^*, the admittance Y^* and the permittivity ε^*. With the appropriate data analysis, it is possible to characterize the different electrically active regions in a material by demonstrating their existence and by measuring their individual electric properties.

To check the quality of the impedance data, what is essential for a proper CNLS analysis, the Kramers-Kronig (K-K) validation tests were performed in the present study with the use of computer program by Boukamp [15,16]. A random distribution of the real part of the relative differences (red dots) and the imaginary part of the relative differences (blue dots) between the measured and calculated values (residuals) around the frequency axis indicates that the data are K-K compliant. One can see that in the present study the deviation is less than 2% (Fig.4). Combination of the measured data (open circles) and its K-K transformation (crosses) shown in Fig.4 proves a good quality of the measured impedance data of BNFO ceramics.

Contribution of microscopic elements such as grain, grain boundaries to total dielectric response in crystalline solids can be identified by a reference to an equivalent circuit, which contains a series of array of parallel RC elements. In order to extract from impedance measurements as much information as possible, the experimental spectra were subjected to CNLS fitting procedure with ZView (Scribner Associates, Inc.) computer program. Equivalent circuit used for impedance spectroscopy data simulation in the present study was composed of resistors (R), capacitive element of constant phase (CPE) and Warburg impedance element (W). R2 and CPE2 elements connected in parallel can be attributed to phenomena present on the material sample – electrode interface. Part of the circuit consisting of resistor R1, CPE1 element and Warburg impedance element (W) can be attributed to the phenomena that occur in the bulk of the sample. Application of a Warburg impedance made it possible to take into account the diffusion of ions in the material sample. An equivalent electric circuit used for impedance data simulation and fitting in the present study is given in Fig. 5. Results of the data simulation are given in Tab. 2.

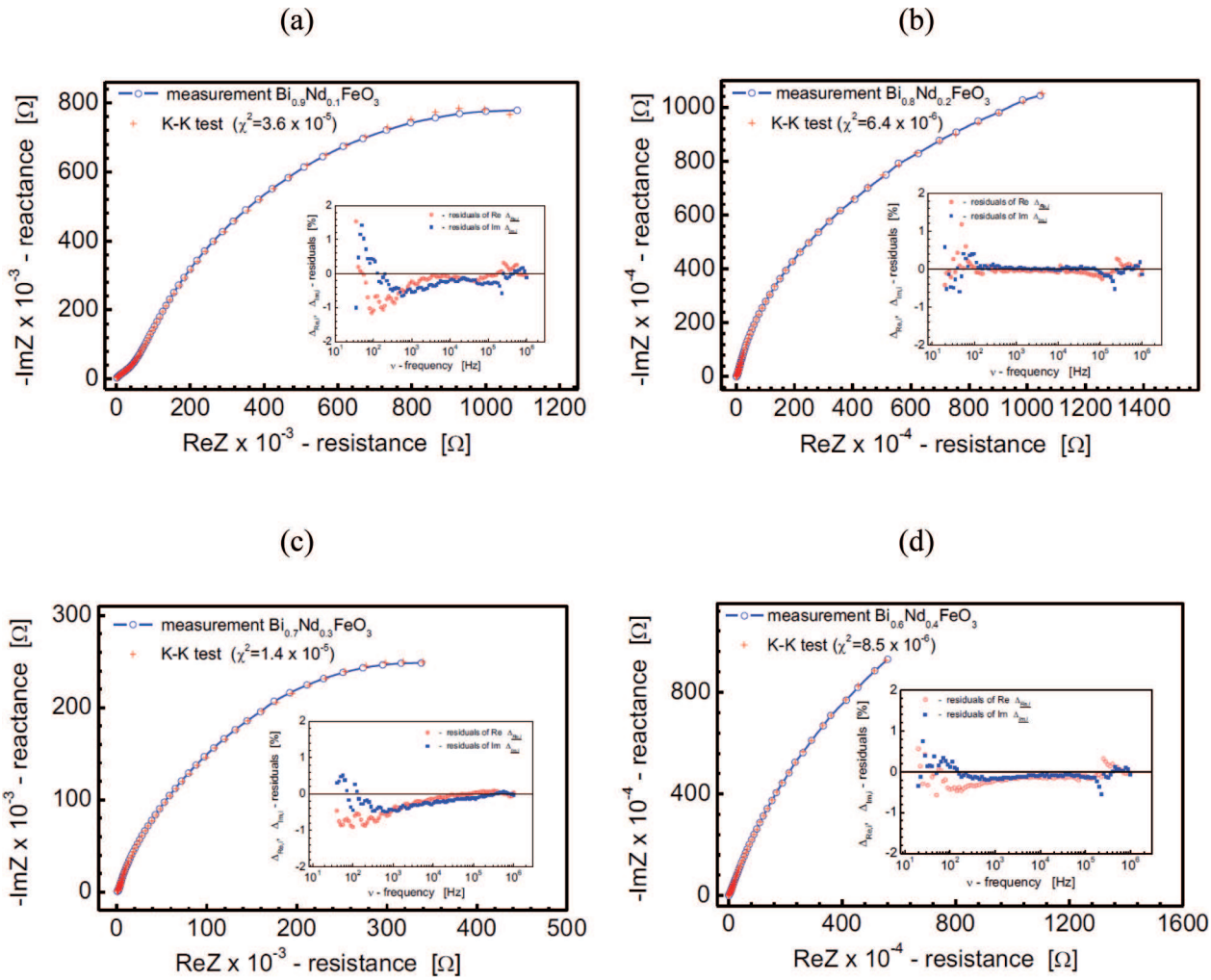

Fig. 4. Impedance diagram for $Bi_{0.9}Nd_{0.1}FeO_3$ (a), $Bi_{0.8}Nd_{0.2}FeO_3$(b), $Bi_{0.7}Nd_{0.3}FeO_3$(c), $Bi_{0.6}Nd_{0.4}FeO_3$(d), open circles, measured data, crosses, Kramers-Kronig transform test results. The insets show results of the K-K test in the form of the relative differences plot

TABLE 2

Estimated values of R, CPE and Warburg impedance element calculated from equivalent electric circuit given in Fig. 5. The validity of the fitting procedure was estimated by $\chi 2$ and WSS

	$Bi_{0.9}Nd_{0.1}FeO_3$	*Error [%]*	$Bi_{0.8}Nd_{0.1}FeO_3$	*Error [%]*	$Bi_{0.7}$ $Nd_{0.3}FeO_3$	*Error [%]*	$Bi_{0.6}Nd_{0.4}FeO_3$	*Error [%]*
W1-R[Ω]	$3.77{\cdot}10^{5}$	5.92	$1.22{\cdot}10^{6}$	17.08	8728	23	$6.1{\cdot}10^{5}$	7.97
W1-T[1]	$2.35{\cdot}10^{-3}$	6.41	$1.35{\cdot}10^{-3}$	5.58	$3.5{\cdot}10^{-4}$	7.13	$4.31{\cdot}10^{-3}$	6.01
W1-P[1]	0.47	1.61	0.67	3.32	0.65	4.5	0.5	1.5
R1[Ω]	28295	3.77	32719	12.71	1225	2.37	14073	7.93
CPE1-T[F]	$1.87{\cdot}10^{-9}$	8.43	$4.79{\cdot}10^{-9}$	26.83	$1.43{\cdot}10^{-8}$	30	$2.97{\cdot}10^{-10}$	11.79
CPE1-P[1]	0.74	0.68	0.69	2.26	0.71	2.56	0.93	0.82
R2[Ω]	$1.71{\cdot}10^{6}$	3.18	$2.53{\cdot}10^{7}$	1.68	$6.66{\cdot}10^{5}$	1.52	$4.23{\cdot}10^{7}$	2.14
CPE2-T[F]	$4.92{\cdot}10^{-9}$	8.09	$6.97{\cdot}10^{-10}$	2.89	$1.58{\cdot}10^{-8}$	3.68	$1.4{\cdot}10^{-9}$	1.71
CPE2-P[1]	0.91	1.80	0.87	0.72	0.8	0.81	0.84	0.
WSS	0.02	–	0.02	–	0.02	–	0.007	–
χ**2**	$1.3{\cdot}10^{-4}$	–	$1.66{\cdot}10^{-4}$	–	$1.63{\cdot}10^{-4}$	–	$4.37{\cdot}10^{-5}$	–

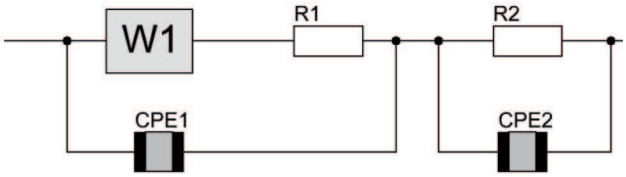

Fig. 5. Schematic representation of the equivalent circuit used in the dispersion analysis of $Bi_{1-x}Nd_xFeO_3$ ceramics

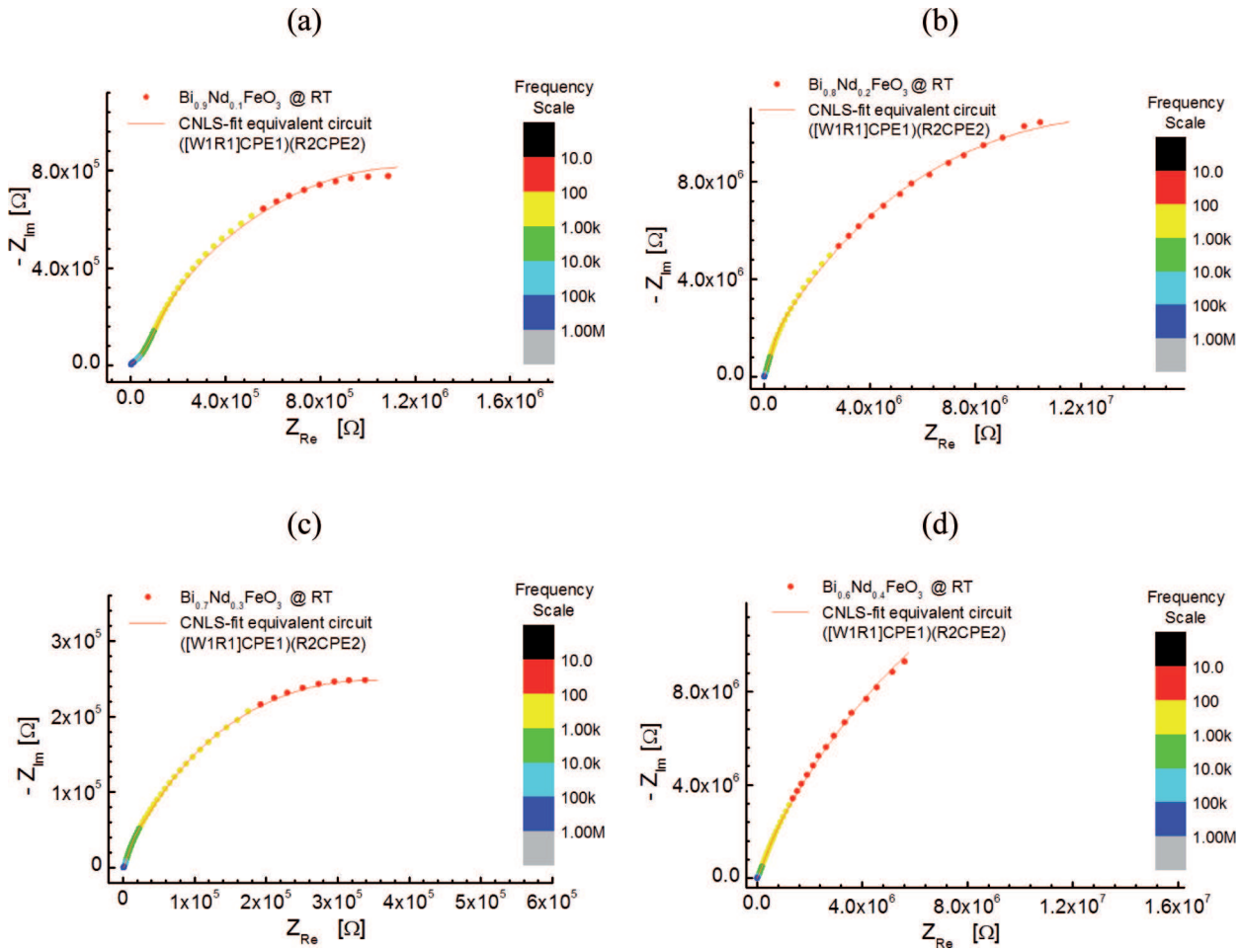

Fig. 6. Plot of Z'' vs. Z' for $Bi_{0.9}Nd_{0.1}FeO_3$ (a), $Bi_{0.8}Nd_{0.2}FeO_3$(b), $Bi_{0.7}Nd_{0.3}FeO_3$(c), $Bi_{0.6}Nd_{0.4}FeO_3$(d). Combination of the measured data (circles) and its CNLS-fit (line) is given

The combination of the measured data (i.e., the real part Z' and imaginary part Z'' of the complex impedance with frequency at room temperatures) and its CNLS-fit in a complex Z''–Z' plane are given in Fig.6 a,b,c,d, for different compositions. As a quality fit parameter the value of the weighted sum of squares (WSS) and χ – square (chi-square), were used (Tab. 2). One can see that numerical characteristics (weighted sum of squares and χ – square) show good agreement between the impedance spectra of BNFO ceramics and dielectric response of a supposed electric model.

4. Conclusions

In the present study $Bi_{1-x}Nd_xFeO_3$ ceramics has been fabricated by mixed oxide method from the stoichiometric mixture of oxides, viz Bi_2O_3, Nd_2O_3 and Fe_2O_3. Simultaneous thermal analysis made it possible to determine temperature of calcination an sintering. SEM micrographs of $Bi_{1-x}Nd_xFeO_3$ ceramics sintered at T=1000°C for t=24h show that neodymium concentration had a significant influence on the grain growth. An increase in Nd content caused a decrease in the average size of the ceramics grains. Crystalline structure of $Bi_{1-x}Nd_xFeO_3$ ceramics for $x \leqslant 0{,}2$ was decribed

by rhombohedral symmetry whereas for $x \geqslant 0{,}3$ by orthorhombic symmetry.

The equivalent electric circuit used in the present study consisted of a series combination of two parallel (R, CPE) circuit. The use of a Warburg impedance element in one of the (R, CPE) circuits made it possible to take into account the diffusion of ions in the ceramics material. The experimental response was found in good agreement with the simulated one thus indicating that the proposed model gave an adequate representation of the electrical properties of the BNFO ceramic sample at room temperature.

Acknowledgements

The present research has been supported by Polish Ministry of Education and Science from the funds for science in 2008-2011 as a research project N N507 446934.

REFERENCES

[1] J.-M. Liu, Q.C. Li, X.S. Gao, Y. Yang, X.H. Zhou, X.Y. Chen, Z.G. Liu, Order coupling in ferroelectromagnets as simulated by a Monte Carlo method, Phys. Rev. **B 66**, 054416, 1-11 (2002).

[2] N.A. Hill, Why Are There so Few Magnetic Ferroelectrics?, J. Phys. Chem. **B 104**, 6694-6709 (2000).

[3] J. Wang, J.B. Neaton, H. Zheng, V. Nagarajan, S.B. Ogale, B. Liu, D. Viehland, V. Vaithyanathan, D.G. Schlom, U.V. Waghmare, N.A. Spaldin, K.M. Rabe, M. Wuttig, R. Ramesh, Epitaxial $BiFeO_3$ Multiferroic Thin Film Heterostructures, Science 299, 1719 (2003).

[4] G.A. Smolenskii, V.A. Isupov, A.I. Agranovskaya, N.N. Krainik, Sov., New ferroelectrics of complex composition IV, Phys. Solid State **2**, 2651 (1961).

[5] K. Takahashi, N. Kida, M. Tonouchi, Phys Rev Lett **96**, 117402 (2006).

[6] V.L. Mathe, K.K. Patankar, R.N. Patil, C.D. Lokhande, Synthesis and dielectric properties of $Bi_{1-x}Nd_xFeO_3$ perovskites, Journal of Magnetism and Magnetic Materials **270**, 3, 380-388 April (2004).

[7] G.L. Yuan, Or D. Siu-wing, L. Helen, W. Chan, Raman scattering spectra and ferroelectric properties of $Bi_{1-x}Nd_xFeO_3$ (x=0-0.2) multiferroic ceramics, Journal of Applied Physics **101**, 064101 (2007).

[8] A. Belsky, M. Hellenbrandt, V.L. Karen, P. Luksch, Crist Acta. **B58**, 364-369 (2002).

[9] B. Boukamp, A Nonlinear Least Squares Fit procedure for analysis of immittance data of electrochemical systems, Solid State Ionics **20**, 31-44 (1986).

[10] P. Zoltowski, Non-traditional approach to measurement models for analysis of impedance spectra, Solid State Ionics **176**, 1979-1986 (2005).

[11] A. Lisińska-Czekaj, D. Czekaj, Synthesis of $Bi_5TiNbMO_{15}$ ceramics, Archives of Metallurgy and Materials **54**, 4, 869-874 (2009).

[12] L. Kozielski, M. Adamczyk, Electrical and mechanical examination of PLZ graded structure for photovoltaic driven piezoelectric transformers **54**, 4, 973-978 (2009).

[13] E. Barsukov, J. Ross Macdonald, (Red.), Impedance spectroscopy, theory, experiment, and applications, John Willey &Sons, Inc., Hoboken, New Jersey, (2005).

[14] W. Bogusz, F. Krok, Elektrolity stałe. Właściwości elektryczne i sposoby ich pomiaru, WNT Warszawa (1995).

[15] B.A. Boukamp, Electrochemical impedance spectroscopy in solid state ionics; Recent advances, Solid State Ionics **169**, 1-4, 65-73 (2004).

[16] B.A. Boukamp, A linear Kronig–Kramers transformation test for immitance data validation, Journal of the Electrochemical Society **142**, 6, 1885-1894 (1995).

Received: 20 March 2011.